Eur. Phys. J. C (2025) 85:125
https://doi.org/10.1140/epjc/s10052-025-13854-2

THE EUROPEAN PHYSICAL JOURNAL C

Regular Article - Theoretical Physics

Exhibiting stable model of dark energy compact star with Tolman-VI solution under complexity free system

Hammad Nazar[1,2,a], **Abdul Majeed**[1,b], **Ghulam Abbas**[1,c], **Asifa Ashraf**[3,d], **Phongpichit Channuie**[4,5,e]

[1] Department of Mathematics, The Islamia University of Bahawalpur, Bahawalpur 63100, Pakistan
[2] Research Center of Astrophysics and Cosmology, Khazar University, 41 Mehseti Street, 1096 Baku, Azerbaijan
[3] School of Mathematical Sciences, Zhejiang Normal University, Jinhua 321004, Zhejiang, China
[4] School of Science, Walailak University, Nakhon Si Thammarat 80160, Thailand
[5] College of Graduate Studies, Walailak University, Nakhon Si Thammarat 80160, Thailand

Received: 10 December 2024 / Accepted: 19 January 2025

Abstract Several recent developments have highlighted the significance of the vanishing complexity factor formalism in understanding the structure and evolution of stellar relativistic compact objects. This formalism, introduced through a novel definition proposed by Herrera (Phys. Rev. D 97:044010, 2018), offers valuable insights into the dynamics of such systems. In this manuscript, we explored a class of realistic solutions to the static and spherically symmetric field equations characterized by two fluid distributions: ordinary stellar matter and dark energy, within the framework of this formalism. Utilizing the well-known Tolman-VI solution as the seed ansatz for the metric coefficient g_{rr}, we employed the complexity-free format to derive an analytic solution for the other metric coefficient, g_{tt}. Subsequently, we obtained the solutions of gravitational field equations for our proposed spacetime model by incorporating the linear dark energy equation of state. These results were applied to the astrophysical compact star candidate $LMC\ X$-4, with $M = 1.04M_{\odot}$ and $R = 8.4$ km. The potential viability and credibility of the proposed dark star solutions were thoroughly analyzed by examining key constraints, including the regularity of metric functions, physical adequacy through matter variables, state parameter behavior, energy conditions, stability tests (such as pressure anisotropy and hydrostatic equilibrium), the speed of sound, and the mass–radius relation for this compact star candidate. Notably, the estimated values of the dark energy coupling factor, presented in Table 1, highlight the exotic nature of the fluid distribution and effectively quantify the contribution of dark energy to the structure and evolution of an ultra-relativistic dark compact star. These findings strongly support our model solutions and demonstrate improvements over previously reported results in Rej et al. (Chin J Phys 87:608, 2024).

1 Introduction

General Relativity (GR), introduced by Albert Einstein, is one of the most remarkable theories for explaining the gravitational interaction between spacetime-geometry and the distribution of matter [1]. It provides the fundamental equations of motion necessary to understand the stability of energy content in cosmological and astrophysical systems on large scales. Experimental tests of GR effectively elucidate and provide precise insights into phenomena such as the deflection of light near massive objects and the motion of dynamic structures within strong gravitational fields, including those around neutron stars, pulsars, and black holes. An additional consequence of GR, affirmed through empirical evidence and active research, is the discovery of gravitational waves. Neutron stars and other compact objects (COs) are promising candidates for studying and testing the viability of GR. The field equations derived from GR establish a connection between geometric functions, also known as gravitational potentials, and the matter distribution. The determination of the matter content often depends on the choice of convenient geometrical methods. For spacetime geometries characterized by two gravitational potentials, the most common approach involves fixing one potential and subsequently solving for the remaining metric function. This pro-

[a] e-mails: hammadnazar350@gmail.com; hamad.nazar@khazar.org
[b] e-mail: prof.abdulmajeedpgckotadu@gmail.com
[c] e-mail: ghulamabbas@iub.edu.pk
[d] e-mail: asifamustafa3828@gmail.com
[e] e-mail: phongpichit.ch@mail.wu.ac.th (corresponding author)

Published online: 01 February 2025

cedure frequently incorporates the equation of state (EoS) [2–4] or imposes constraints on matter variables, such as pressure isotropy [5]. Recently, the vanishing complexity factor condition [6] has also gained significant attention. Additionally, this approach may involve the so-called Karmarkar condition, which embeds the curvature tensor within a five-dimensional flat metric [7,8].

In recent times, Herrera's [9] proposed complexity factor condition has emerged as a supplementary tool for constraining matter distribution, potentially serving as an alternative to implementing EoS. Interestingly, this approach can account for the complexity factor in both static and dynamical systems [9,10]. Consequently, it provides a framework for studying the structural properties and evolution of self-gravitating bodies, including models of ultra-relativistic COs. Notably, the complexity factor condition introduces an additional relationship that links the principal matter terms derived from the energy–momentum tensor. These terms include energy density, pressures, shear stresses, and heat flux, particularly in scenarios involving dynamical and dissipative collapse. The definition of complexity based on these bulk properties differs significantly from the original concept, which was rooted in the notions of information and disequilibrium, as defined through statistical analysis [11,12]. This concept has also been applied to the modeling of self-gravitating COs [13–16]. In contrast, a quite recent study has redefined the term "complexity" through Herrera's pioneering work [9], which proposed a novel interpretation for static and spherically symmetric self-gravitating systems. This redefinition focuses on the combination of key matter terms, such as the inhomogeneity of energy density and pressure anisotropy, as they appear in the structure scalars derived through the orthogonal splitting of the curvature tensor. The orthogonal splitting of the curvature tensor for formulating structure scalars was initially introduced by Bel [17] and subsequently reviewed by Gómez-Lobo [18] and Herrera et al. [19]. Building on these foundations, the new complexity factor condition provides an intuitive framework for understanding the structure and evolution of astrophysical COs. Specifically, it can be applied to constrain such systems by employing the vanishing complexity factor condition. The concept of the complexity factor was initially introduced from a mathematical perspective to describe the physical parameters governing the generation of complexity in relativistic self-gravitating systems. However, its significance became evident when it was employed as an additional criterion for analyzing the structural equations required to achieve hydrostatic equilibrium. The study of complexity in the realm of relativistic astrophysical COs has garnered significant attention, leading to the development of several novel approaches for deriving their interior solutions within the framework of GR and modified theories of gravity. These solutions are crucial for understanding the physical properties, structure, and evolution of self-gravitating compact geometries [20–37]. Notably, the introduction of the complexity factor offers a framework in which constraints like pressure isotropy, energy density homogeneity, and the imposition of EoS can be bypassed [38]. In particular, the complexity factor serves as a self-consistent mechanism for incorporating anisotropy into the analysis. The effectiveness of applying the vanishing complexity condition has been demonstrated in recent studies, even for systems governed by modified and higher-order gravity theories [39–54].

We investigate the concept of the vanishing complexity factor for static and anisotropic spherically symmetric stars surrounded by a two-fluid distribution, namely, normal baryonic matter and dark energy. In particular, the non-baryonic matter, commonly referred to as dark matter, exhibits a repulsive influence characterized by negative pressure, as described by the dark energy EoS. From this perspective, Lobo [55] explored the stability of interior stellar COs by incorporating the dark energy EoS, which plays a crucial role in understanding the stability of stellar structures and serves as a fundamental component in solving various astrophysical problems. This is particularly evident in the linear EoS with the inclusion of surface density, which leads to physically acceptable and sustainable stellar configurations [56]. Several feasible $EoSs$ originating from particle physics provide valuable insights into the microphysics of such systems. However, deriving exact solutions often requires laborious numerical approaches. For dark energy stars, the EoS is typically expressed as $p = -\rho$, as originally proposed by Gliner [57], with the Bardeen geometry providing the first solution in this context [58]. In some works, Bhar and Rahaman [59] highlighted various physical attributes to analyze the outcomes of Einstein's field equations for the stable formation of dark energy COs. Bhar [60] investigated the implications of isotropic, spherically symmetric compact stars composed of both ordinary stellar matter and dark matter, elaborating that any astrophysical system could potentially serve as a viable candidate for a dark energy star. Abbas et al. [61] explored the feasible characteristics of an anisotropic cylindrical system with a cosmological variable, proposing it as a realistic choice for mimicking dark energy COs. Continuing along this debate, we highlight recent advancements in the modeling of stellar COs within the framework of vanishing complexity formalism. Rej et al. [62] examined the effects of the dark energy coupling parameter on anisotropic compact stellar models under the vanishing complexity factor condition, utilizing the Finch–Skea spacetime solution. Their findings indicate that the coupling parameter allows for minimal features required to align with standard datasets for modeling dark energy star candidates. Using the vanishing complexity condition, Maurya et al. [63] studied the phenomenological implications of gravitational wave echoes for anisotropic and spherically symmetric COs within galactic dark matter halos, employing a

complete deformation geometric approach. Panotopoulos et al. [64] reviewed several realistic properties of stellar dark energy stars using the extended Chaplygin EoS under the vanishing complexity factor condition. Similarly, Rincón et al. [65] investigated the physical characteristics of tidal Love numbers for anisotropic spherical compact bodies by selecting specific anisotropic factors. Numerous research groups have explored various physical aspects of relativistic astrophysical COs, treating them as viable testbeds for mimicking dark energy stellar models. These studies involve diverse geometrical approaches in the context of normal baryonic matter extended with exotic matter and quark-gluon fluids [66–80].

It is undoubtedly established that any proposed ansatz for geometrical spacetime must be physically reliable and free from singularities to ensure the stable interior configuration of relativistic stellar COs. The selection of geometric variables as a seed ansatz to support the essential physical characteristics of a system has long been a subject of debate among researchers. In support of the chosen seed ansatz, several realistic models have been analyzed to confirm the potential viability and sustainability of relativistic stellar systems. In this work, we construct our spacetime results by adopting the Tolman-VI solution as the seed ansatz, combined with the characteristics of a linear dark energy EoS within the framework of the vanishing complexity factor formalism. From this perspective, Tolman [81] was the first to introduce the study of eight distinct geometric variables by independently formulating analytical solutions to the Einstein field equations. Biswas et al. [82] examined the physical acceptability of a relativistic stellar model composed of anisotropic strange quark matter, utilizing the Tolman–Kuchowicz ansatz as the seed solution. Similarly, Jasim et al. [83] investigated the stability of static, anisotropic, spherically symmetric COs under a cosmological constant, employing the strange quark matter MIT bag model and the same ansatz. Biswas et al. [84] constructed feasible solutions to the Einstein field equations using this ansatz to model anisotropic ultra-relativistic COs composed of strange quark matter within the framework of $f(R,T)$ gravity. Majeed et al. [85] applied such metric solutions to model anisotropic compact stars in the context of non-conservative gravity theories. Hansraj and Banerjee [86] explored the physical significance of Tolman metrics for static, spherically symmetric perfect fluid spheres in modified $f(R,T)$ gravity theory, demonstrating that these metric potentials exhibit stable and realistic features for sustainable models. From the literature survey, numerous significant attempts have been made to employ the Tolman ansatz for modeling astrophysical COs within various gravitational theories [87–96].

The outline of our article is as follows: In Sect. 2, we explore the stellar matter distribution of a static and spherically symmetric model, along with the properties of dark energy, to examine the gravitational field equations within the framework of a vanishing complexity factor. Using the Tolman-VI ansatz as a seed solution for the radial metric component, we derive the corresponding temporal metric function under this vanishing complexity condition. In Sect. 3, we extend these spacetime solutions by incorporating the linear dark energy EoS to derive the final expressions for the Einstein field equations. To resolve the unknown constants, we conduct a smooth matching of the interior and exterior spacetimes at the hypersurface, as detailed in this section. Furthermore, in Sects. 4 and 5, we evaluate the physical viability and stability of our proposed dark star model through both graphical and analytical methods. This evaluation encompasses the regularity of metric functions, matter variables, the equation of state parameter, energy conditions, pressure anisotropy, hydrostatic equilibrium, the causality condition, and the mass–radius relation. Finally, in Sect. 6, we present concluding remarks that summarize and highlight the significance of our proposed dark star model.

2 Dark stellar interior matter configuration and fundamental equations

The Einstein field equations primarily describe the gravitational interaction between geometry and the matter field, and they can be expressed in tensorial form as:

$$\mathcal{G}_{\sigma\tau} = R_{\sigma\tau} - \frac{g_{\sigma\tau}R}{2} = 8\pi\mathcal{T}_{\sigma\tau}. \tag{1}$$

In this section, we describe the matter configuration within the stellar interior of a static and locally anisotropic spherically symmetric compact sphere, characterized by a two-fluid distribution consisting of ordinary matter and an exotic fluid known as dark matter. It is a realistic choice to use the standard Schwarzschild-like coordinates (t, r, θ, ϕ) which can be expressed through the following line-element in the comoving frame

$$ds^2 = e^a dt^2 - e^b dr^2 - r^2 d\theta^2 - r^2 \sin^2\theta d\phi^2. \tag{2}$$

The gravitational functions, denoted as $a = a(r)$ and $b = b(r)$, depend solely on the radial coordinate r and are assumed to be positive. The required solutions for both metric functions, provided in the subsequent section, will be utilized to express the analytical solutions of the Einstein field equations in more compact form. Here, we consider the system to be anisotropic, meaning that there is pressure not only in the radial direction (p_r) but also in the transverse direction (p_t). The fluid distribution, characterized by pressure anisotropy, is used to investigate interior solutions for relativistic stellar compact spheres, particularly those with a significant degree of anisotropic fluid. So, the energy–momentum tensor for a

locally anisotropic stellar fluid distribution is defined as

$$\mathcal{T}_{\sigma\tau} = \Big(\rho + p_t\Big)u_\sigma u_\tau - p_t g_{\sigma\tau} + \Big(p_r - p_t\Big)\upsilon_\sigma \upsilon_\tau. \tag{3}$$

Here, the matter components, ρ, p_r and p_t represent the energy density, radial pressure, and tangential pressure, respectively. Additionally, u^σ denotes the fluid four-velocity vector, while υ^σ is the unit space-like vector in the radial direction. The effective energy–momentum tensor for a relativistic compact sphere is influenced by a two fluid distribution, generally comprising normal baryonic matter along with the contribution of dark energy components, characterized by energy density ρ^{de}, radial pressure p_r^{de}, and transverse pressure p_t^{de}, as defined below

$$\mathcal{T}_{00} = \rho^{(eff)} = \rho + \rho^{de}, \tag{4}$$

$$\mathcal{T}_{11} = -p_r^{(eff)} = -\Big(p + p_r^{de}\Big), \tag{5}$$

$$\mathcal{T}_{22} = \mathcal{T}_{33} = -p_t^{(eff)} = -\Big(p + p_t^{de}\Big). \tag{6}$$

The Einstein field equations (1) for the line-element (2), combined with the two fluid components (4)–(6), can be derived as follows

$$8\pi\rho^{(eff)} = e^{-b}\left(\frac{b'r + e^b - 1}{r^2}\right), \tag{7}$$

$$8\pi p_r^{(eff)} = e^{-b}\left(\frac{a'r - e^b + 1}{r^2}\right), \tag{8}$$

$$8\pi p_t^{(eff)} = \frac{e^{-b}}{4}\left(a'\Big(a' - b'\Big) + 2a'' + \frac{2}{r}\Big(a' - b'\Big)\right). \tag{9}$$

In the subsequent section, we elaborate on and apply the vanishing complexity condition to determine the analytical form of the metric function. This approach provides an additional geometrical tool for analyzing the structure and evolution of relativistic COs, especially in scenarios where other geometrical methods are not straightforward to implement.

2.1 Applying vanishing complexity factor condition on anisotropic matter configuration

This study provides readers with the necessary ingredients to understand the concept of the vanishing complexity factor condition and its potential applications within the framework of relativistic systems and astrophysical contexts. It is widely recognized that solving the anisotropic interior geometries of celestial objects requires an auxiliary condition to fully close the system. Among the various methods available to address this requirement, we adopt the concept of complexity, as proposed in [9], for static and spherically symmetric self-gravitating systems. This approach introduces a fresh perspective on complexity, addressing two major shortcomings of earlier concepts. Previous approaches offered a limited understanding of the energy density fluid by focusing solely on energy density while neglecting other critical factors, such as pressure. Additionally, these earlier models modified the probability distribution with the energy density of the fluid distribution, as highlighted in [15].

The vanishing complexity factor condition offers an alternative approach to addressing anisotropies in the modeling of (CO) [93,97–99]. This condition, based on the orthogonal decomposition of the curvature tensor, yields trace-free results expressed in terms of scalar functions. These scalars are closely linked to the kinematic and physical properties of the fluid [100]. Furthermore, it is important to note that, for static anisotropic matter configurations, the complexity factor condition serves as a geometric framework for formulating EoS that relate radial and tangential pressures. In the context of studying the complexity factor for static, self-gravitating celestial objects, it is well-established that a homogeneous isotropic fluid represents one of the simplest systems, as it serves as a baseline for measuring deviations from complexity. Thus, the complexity factor is expected to evaluate the relationship between energy density inhomogeneity and pressure anisotropy within a system. This study provides a concise overview of the complexity factor formalism and highlights its significance in astrophysical research. The complexity factor function (Y_{TF}) has been extensively studied, and no additional framework is needed here for its formulation. The scalar function of the complexity factor is expressed as follows:

$$Y_{TF} = 8\pi\,\Pi - \frac{4\pi}{r^3}\int_0^r \left(\rho^{(eff)}(r)\right)' r^3 dr. \tag{10}$$

It highlights the fundamental significance of the simplest configuration, determined by the system's energy density in conjunction with isotropic pressure. Specifically, this corresponds to a system sustained by a homogeneous isotropic fluid, where any inhomogeneous energy density cancels out the pressure anisotropy [9]. In particular, $Y_{TF} = 0$ indicates that the system is in a state of vanishing complexity. Notably, the complexity factor Y_{TF} deviates for any system where

$$\Pi = \frac{1}{2r^3}\int_0^r \left(\rho^{(eff)}(r)\right)' r^3 dr. \tag{11}$$

This implies the existence of a class of results that validate the applicability of this approach. By applying condition (11), we can establish a feasible bound for the proposed model while solving (1), as it involves a non-local EoS. Through algebraic manipulation of the Einstein field equations, Eq. (10) has been derived as follows:

$$Y_{TF} = \frac{e^{-b}\Big(a'(rb' - ra' + 2) - 2ra''\Big)}{4r}. \tag{12}$$

Using $Y_{TF} = 0$, the result becomes,

$$a'\Big(rb' - ra' + 2\Big) - 2ra'' = 0. \tag{13}$$

The above expression can be written in the form of a total derivative as follows,

$$\frac{d}{dr}\left(\ln a' + \frac{a-b}{2} - \ln r\right) = 0. \tag{14}$$

After integration, we obtain

$$\ln a' + \frac{a-b}{2} - \ln r = \text{constant}. \tag{15}$$

The result in (15) provides a more compact analytical expression for the relationship between a and b following the integration process. From this, we derive

$$e^{\frac{a}{2}} = A\int re^{\frac{b}{2}}dr + B, \tag{16}$$

where A and B are integration constants. For convenience, the above equation can be rewritten as

$$e^{a} = \left(A\int re^{\frac{b}{2}}dr + B\right)^2. \tag{17}$$

It is noteworthy that the result in (17) was first proposed by Contreras and Stuchlík [6].

3 Tolman VI solution in context of vanishing complexity formalism

To develop a potentially sustainable model for ultra-relativistic compact stellar spheres, it is essential to derive exact analytical solutions to the gravitational field equations. These solutions must be feasible and realistic for the static stellar inner core, which is expected to model relativistic astrophysical star formations composed of ordinary baryonic matter combined with dark energy. Constructing authentic solutions to the Einstein field equations is notoriously difficult due to their highly non-linear, second-order differential equations. In this study, we adopt a well-defined spacetime potential based on the Tolman-VI solution as the seed ansatz. This solution has been shown to yield viable implications for relativistic stellar interior configurations in both astrophysical and cosmological contexts. Thus, we utilize the g_{rr} component of the spacetime geometry as the Tolman-VI ansatz, expressed as

$$e^{b} = 2 - n^2. \tag{18}$$

In context of vanishing complexity formalism, and using the relation (17), we obtain the g_{tt} component of the spacetime model as

$$e^{a} = \left(\frac{Ar^2\sqrt{2-n^2}}{2} + B\right)^2. \tag{19}$$

Using the solutions provided in (18) and (19), we derive the necessary expressions for the field equations in terms of the effective matter components as

$$\rho^{eff} = \frac{1-n^2}{8\pi r^2(2-n^2)}, \tag{20}$$

$$p_r^{eff} = \frac{2B(n^2-1) + Ar^2(-2+3n^2-n^4+4\sqrt{2-n^2})}{8\pi r^2(2-n^2)(2B+Ar^2(2-n^2))}, \tag{21}$$

$$p_t^{eff} = \frac{A^2r^2(2-n^2) + 2AB\sqrt{2-n^2}}{2\pi(2-n^2)(2B+Ar^2(2-n^2))^2}. \tag{22}$$

The underlying field equations describing the interior relativistic geometry, composed of two fluid distributions-namely dark matter and normal baryonic matter-are presented in Eqs. (20)–(22). This set of equations consists of three independent equations with five unknown quantities: ρ, ρ^{de}, p, p_r^{de}, and p_t^{de}. To address the challenge of solving this underdetermined system with only three independent equations, two additional constraints are required. To balance the system, we assume a linear dark energy EoS. The system of equations (20)–(22) is then solved by employing methods developed in prior research, as outlined in [101–111], where the exotic nature of dark energy aids in configuring relativistic compact objects (COs). In this framework, the radial pressure of dark energy (p_r^{de}) is proportional to the dark energy density (ρ^{de}), while the dark energy density is proportional to the ordinary stellar matter density (ρ), i.e.,

$$p_r^{de} = -\rho^{de}, \tag{23}$$

$$\rho^{de} = \alpha\rho. \tag{24}$$

Here, α is a proportionality constant treated as the dark energy coupling parameter, whose value can be determined from the matching conditions. It is important to note that the dark energy EoS given in (23)–(24) indicates that the matter configuration under consideration is exotic in nature. Consequently, this matter distribution is often referred to as a "degenerate vacuum" or "fallacious vacuum". By substituting Eqs. (23)–(24) into the set of Eqs. (20)–(22), we derive the components corresponding to ordinary stellar matter and dark energy as

$$\rho = \frac{1-n^2}{8\pi(\alpha+1)\left(2-n^2\right)r^2}, \tag{25}$$

$$p = \frac{Ar^2\left(-n^4+4\alpha\sqrt{2-n^2}+3n^2+4\sqrt{2-n^2}-2\right)+2B\left(n^2-1\right)}{8\pi(\alpha+1)\left(2-n^2\right)r^2\left(A\left(2-n^2\right)r^2+2B\right)}, \tag{26}$$

and

$$\rho^{de} = \frac{\alpha\left(1-n^2\right)}{8\pi(\alpha+1)\left(2-n^2\right)r^2}, \tag{27}$$

$$p_r^{de} = -\frac{\alpha\left(1-n^2\right)}{8\pi(\alpha+1)\left(2-n^2\right)r^2}, \tag{28}$$

$$p_t^{de} = \frac{-4ABr^2(-n^4+4\alpha\sqrt{2-n^2}+3n^2+4\sqrt{2-n^2}-2)-4B^2(n^2-1)+\gamma_1}{8\pi(\alpha+1)(n^2-2)(A(n^2-2)r^3-2Br)^2}. \tag{29}$$

where,

$$\gamma_1 = A^2\left(n^2-2\right)r^4\left(-n^4+4\alpha\left(\sqrt{2-n^2}+1\right)+3n^2+4\sqrt{2-n^2}+2\right).$$

Next, we determine the values of the unknown constants involved in the spacetime solutions by applying the matching constraints between the inner geometry and the outer metric at the boundary hypersurface, where $r = R$ with R representing the radius of the star. We employ the conventional method of smooth matching at the junction interface between the interior and exterior geometries to compute the values of these unknown constants. For this purpose, we adopt the Schwarzschild vacuum solution as the exterior line element [112], given as follows:

$$ds^2 = F(r)dt^2 - \left(F(r)\right)^{-1}dr^2 - r^2\left(d\theta^2+sin^2\theta d\phi^2\right). \tag{30}$$

Here, $F(r) = \left(1-\frac{2M}{r}\right)$, where M denotes the total mass of the dark energy star. The matching constraints for both metrics ensure the continuity of g_{tt} and g_{rr} at the boundary surface, which is governed by the Israel–Darmois junction conditions [113,114]. Accordingly, these constraints lead to the following relationship

$$\left(\frac{AR^2\sqrt{2-n^2}}{2}+B\right)^2 = \left(1-\frac{2M}{R}\right), \tag{31}$$

$$\left(2-n^2\right) = \left(1-\frac{2M}{R}\right)^{-1}. \tag{32}$$

From the above expression, the values of the unknown constants can be determined as follows

$$n = +\sqrt{\frac{R-4M}{R-2M}}, \tag{33}$$

$$B = \frac{\sqrt{R-2M}}{\sqrt{R}} - \frac{1}{2}A\sqrt{2-n^2}R^2. \tag{34}$$

As a result, we determined the required forms of the unknown constants n and B in terms of the total mass M and radius R corresponding to the well-known astrophysical compact star candidate $LMC\ X$-4, with $M = 1.04M_\odot$ and $R = 8.4$ km [115]. It is important to note that the dimensions of the unknown constants A, B and n are km^{-2}, km^0 and km^0, respectively. The dark energy coupling parameter α is also calculated using the condition of vanishing radial pressure at the star's surface, i.e., $(p_r(r = R) = 0)$, and is expressed as

$$\alpha = \frac{A\left(n^4-3n^2-4\sqrt{2-n^2}+2\right)R^2-2B\left(n^2-1\right)}{4A\sqrt{2-n^2}R^2}. \tag{35}$$

The numerically computed values of these unknowns, corresponding to the viable compact star $LMC\ X$-4, are given in Table 1.

Table 1 Numerical values of the constants A, B, n, along with the dark energy coupling parameter α, are presented for the dark energy star model $LMCX-4$

A	B	n	α
0.0025	0.686015	0.651618	0.07195
0.0060	0.531030	0.651618	−0.53194
0.0095	0.376044	0.651618	−0.69086
0.00130	0.221059	0.651618	−0.76421

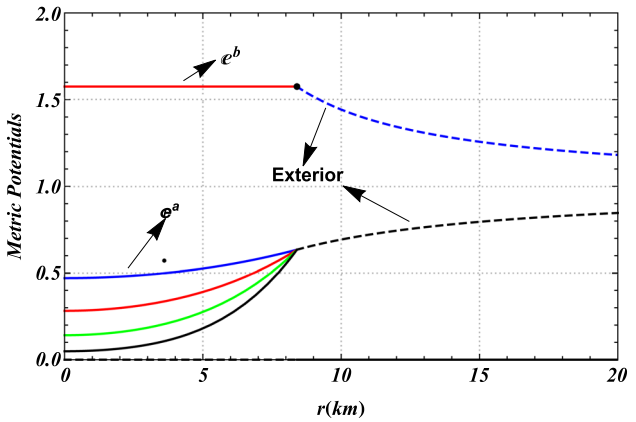

Fig. 1 Physical behavior of the interior geometrical potentials e^a and e^b, alongside the matching of exterior metric functions, as a function of radial distance r for the dark energy star candidate $LMCX-4$

4 Viability of proposed solutions via matter variables

To validate whether the proposed solutions represent a physically sustainable model of a stellar relativistic dark energy star, we have subjected them to rigorous physical conditions in this section. This includes examining the acceptability of non-singularity and the potential regularity of the entire stellar interior configuration by testing the matching of spacetime potentials, matter variables, gradient functions, state parameters, and energy conditions. Through a series of graphical plots, we illustrate the behavior of gravitational and thermodynamic variables, enabling the reader to comprehend the substantial features of the presented model.

4.1 Acceptability of geometric functions

Both metric components are free from central singularities and remain feasible and regular throughout the entire configuration of the dark energy sphere ($r < R$). Additionally, for the presented system, we have $e^{a(0)} = B$, where B is a non-negative constant, and $e^{b(0)} =$ constant.

- As shown in Fig. 1, both geometric components remain non-negative and regular across the entire interior domain of the CO. The physical analysis confirms that the metric functions are devoid of irregularities and central singularities. Furthermore, it is important to note that the interior and exterior metric components are smoothly matched at the boundary hypersurface. These properties collectively underscore the potential viability and sustainability of our proposed model solutions.

4.2 Physical plausibility of density, pressure and gradient functions

The matter components play a pivotal role in assessing the physical credibility and potential viability of the interior configuration of any stellar model. To achieve this, we present our results for the spacetime geometry under consideration by analyzing the matter variables associated with two fluid distributions: ordinary stellar matter and dark energy. Additionally, we examine the effectiveness of these fluids through detailed graphical representations.

- It is crucial to study the structural properties of energy density and pressure, ensuring they remain physically realistic and non-singular throughout the stellar interior (CO) for well-consistent and stable equilibrium star formation. From Fig. 2, we analyze the effects of energy density (left panel) and pressure (right panel) associated with ordinary stellar matter on the proposed star candidate, $LMCX-4$, for various choices of the free parameter A. The results clearly indicate that these quantities exhibit a positive impact and maintain non-singular behavior at every point within the compact sphere. Both energy density and pressure achieve their maximum finite values at the stellar core ($r \sim 0$), reflecting the ultra-relativistic nature of dense COs [116–118]. Additionally, it is important to note that the pressure must vanish at the boundary ($r = R$). Both quantities decrease smoothly with increasing radial coordinate r and approach zero at the surface of the CO (see Fig. 2).

- We analyze the influence of dark energy on the presented star model by examining various matter quantities in Fig. 3. The left panel, depicting the energy density associated with dark energy, shows a decreasing and negative impact throughout the stellar interior (CO). This behavior reflects the intrinsic nature of dark energy, which arises due to the dark energy coupling parameter directly involved in its equation of state (EoS). In other words, this characteristic highlights the exotic nature or repulsive force that emerges in the system as a result of the coupling parameter, with its numerical values provided in Table 1 for the readers reference. Recent studies have similarly noted that the energy density associated with dark energy exhibits a negative influence, attributed to the coupling parameter [119]. Regarding the pressure terms of dark energy, these display positive and non-singular behavior across the entire domain of the compact star (see the right and lower panels of Fig. 3). It is worth mentioning that this impact may arise when the negative pressure effectively counterbalances the negative energy density of dark energy.

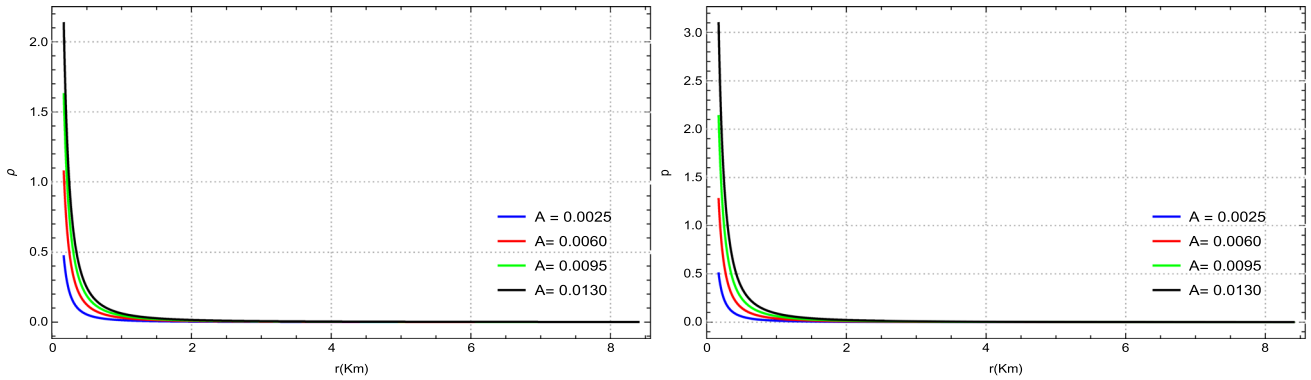

Fig. 2 Profile of energy density (left panel) and pressure (right panel) for ordinary stellar matter versus r

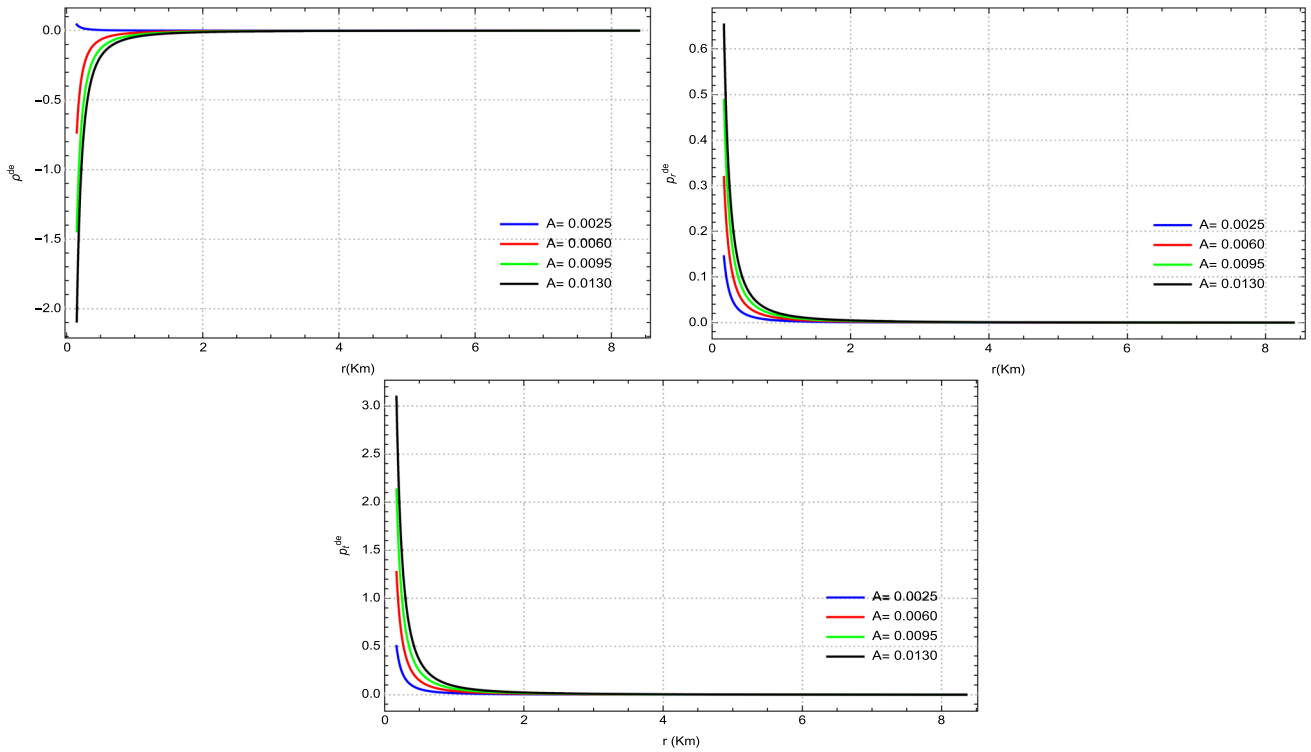

Fig. 3 Variation of energy density (left panel), radial pressure (right panel), and transverse pressure (lower panel) owing to dark energy vs radial function r

- On the other hand, we also examine the effective terms of the matter distribution in Fig. 4. As evident from Fig. 4 (left panel), the energy density due to effective matter demonstrates a positive and regular behavior throughout the entire composition of the compact sphere. It reaches its maximum value at the central core and gradually decreases as the radial distance r increases. In contrast, both pressures arising from effective matter do not exhibit a positive nature and remain decreasing functions of the radial coordinate r across the entire configuration of the CO (see right and lower panels).
- Furthermore, we validate the stability of our proposed model solutions for the dark energy CO by analyzing the energy density and pressure with respect to their first derivatives. As shown clearly in Fig. 5, the first derivatives of the energy density (left panel) and isotropic pressure (right panel) exhibit a negative trend throughout the fluid sphere, behaving as monotonically decreasing functions of the radial coordinate r. This behavior suggests that both gradient functions confirm the physical stability of the model, further supported by their zero values at the stellar core.

As a result, these diverse characteristics of the matter terms in the two-fluid distributions, analyzed within the framework of the vanishing complexity formalism, validate and standard-

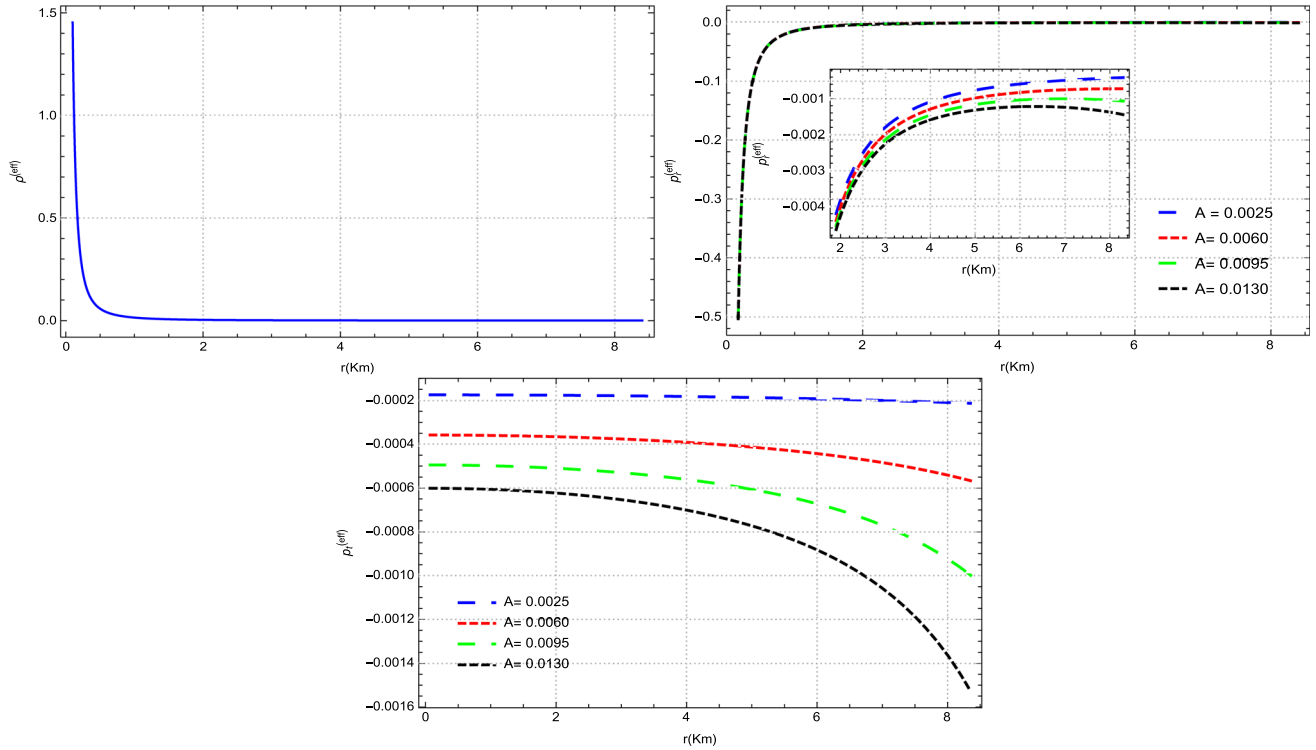

Fig. 4 Physical behavior of energy density (left panel), radial pressure (right panel), and tangential pressure (lower panel) due to effective matter with respect to radial coordinate r

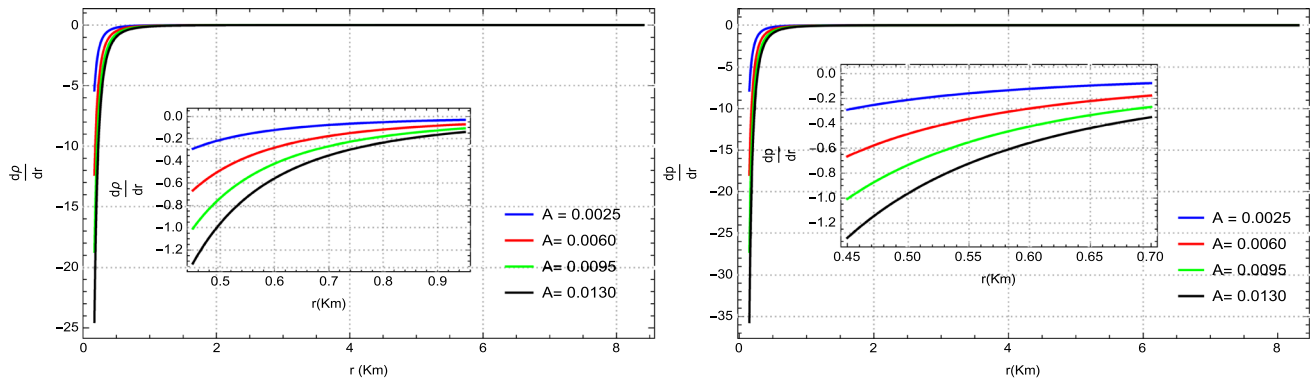

Fig. 5 Physical behavior of gradient functions as a function of r; $\frac{d\rho}{dr}$ (left panel) and $\frac{dp}{dr}$ (right panel)

ize our model solutions. This ensures the configuration of a potentially stable and sustainable dark energy star CO.

4.3 State parameter

The most common form of the EoS is defined as $p = \omega\rho$, where ω represents the parameter for isotropic distribution. Since our study focuses on modeling a dark energy compact star candidate, the state parameter can be expressed as $\omega = \frac{p}{\rho}$, to analyze the structural properties of the stellar interior within the compact configuration ($r < R$). The analytical solution for the state parameter is given by

$$\omega = -\frac{Ar^2\left(-n^4+4(\alpha+1)\sqrt{2-n^2}+3n^2\right)-2Ar^2+2B\left(n^2-1\right)}{\left(n^2-1\right)\left(A\left(n^2-2\right)r^2-2B\right)}. \tag{36}$$

To evaluate the physical adequacy of the state parameter in revealing the structural properties of celestial astrophysical COs, various insights have been derived by analyzing different types of stellar relativistic COs through their EoS parameters [118,120–122].

- In this context, we examine the behavior of the state parameter for the dark energy spherical star model, as depicted in Fig. 6. Figure 6 clearly demonstrates that

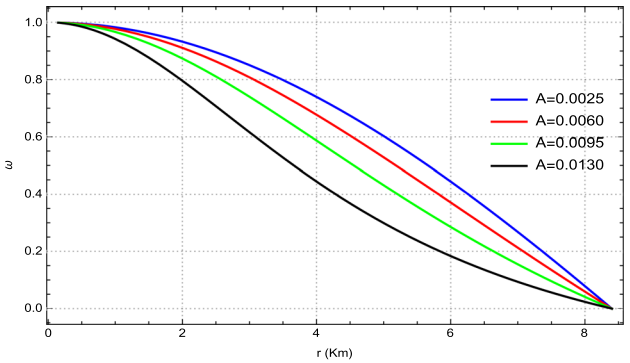

Fig. 6 Physical behavior of state parameter (ω) versus radial function r

the state parameter exhibits a regular and non-singular behavior at every point within the stellar sphere. Notably, it remains positive and adheres to the essential bound, staying within the permissible range $0 \leq \omega \leq 1$). This condition further validates our findings, reinforcing the physical viability and potential equilibrium state of the dark energy CO.

4.4 Energy conditions

It is of utmost importance to reaffirm the physical viability of the fluid distribution within the stellar relativistic CO under various energy conditions. The fluid configuration inside a dark spheroidal object can either be realistic or exotic. For the fluid distribution to be considered realistic, it must satisfy certain constraints related to mass density, radial pressure, and tangential pressure. These constraints are referred to as energy conditions, namely the null energy condition (NEC), weak energy condition (WEC), dominant energy condition (DEC), and strong energy condition (SEC). From this perspective, the following constraints must be satisfied to ensure a physically sustainable dark energy star model. These conditions are expressed as:

$$WEC: \quad \rho^{(eff)} + p_r^{(eff)} \geq 0, \quad \rho^{(eff)} + p_t^{(eff)} \geq 0, \tag{37}$$

$$NEC: \quad \rho^{(eff)} \geq 0, \quad \rho^{(eff)} + p_r^{(eff)} \geq 0, \quad \rho^{(eff)} + p_t^{(eff)} \geq 0, \tag{38}$$

$$DEC: \quad \rho^{(eff)} \geq |p_r^{(eff)}|, \quad \rho^{(eff)} \geq |p_t^{(eff)}|, \tag{39}$$

$$SEC: \quad \rho^{(eff)} + p_r^{(eff)} + 2p_t^{(eff)} \geq 0. \tag{40}$$

- Stabilizing these energy conditions is crucial for substantiating our dark energy compact stellar model. The investigation of the energy conditions mentioned above for both ordinary stellar matter and effective matter distributions, in the context of the compact star $LMCX-4$, is presented in Figs. 7 and 8. These figures demonstrate that all the energy conditions for baryonic and effective matter are satisfied by our model, except for the effective SEC. Notably, the plots of the energy condition profiles indicate optimal behavior at the central stellar region and remain positive across the entire interior domain of the dark energy CO. However, the effective SEC, which corresponds to the two-fluid distribution, reveals an exotic nature characterized by the repulsive action of the dark energy fluid. This suggests that the effective SEC may be significantly influenced by strong gravitational interactions in such scenarios.

5 Stability analysis

To address stellar stability, it is essential to consider several feasible constraints, including pressure anisotropy, force equilibrium, sound speed, and the mass function. The following subsections will provide a detailed analysis of these conditions within the framework of our study.

5.1 Pressure anisotropy

The proposed model must be realistic and adhere to a crucial physical condition regarding pressure anisotropy to ensure a non-singular and stable configuration of the dark energy CO. At the surface ($r = R$), the transverse pressure ($p_t^{(eff)}$) may or may not vanish, but the radial pressure ($p_r^{(eff)}$) must be zero. Pressure anisotropy plays a fundamental role in understanding the unique properties of matter within the core of a stellar system. To calculate the anisotropy in our model, we define it as $\Delta = (p_t^{(eff)} - p_r^{(eff)})$ and proceed to evaluate the pressure anisotropy as follows

$$\Delta = \frac{4B^2\left(-1+n^2\right) - 4ABr^2\left(2-3n^2+n^4\right) + A^2r^4\left(-2+n^2\right)\left(6-3n^2+n^4-4\sqrt{2-n^2}\right)}{8\pi\left(-2+n^2\right)\left(-2Br+Ar^3\left(-2+n^2\right)\right)^2}. \tag{41}$$

For $\Delta > 0$, the pressure anisotropy represents a repulsive force acting outward, while for $\Delta < 0$, it indicates an attractive force acting inward. To evaluate this behavior, we plot the pressure anisotropy as a function of the radial coordinate r for the interior model of the dark energy CO.

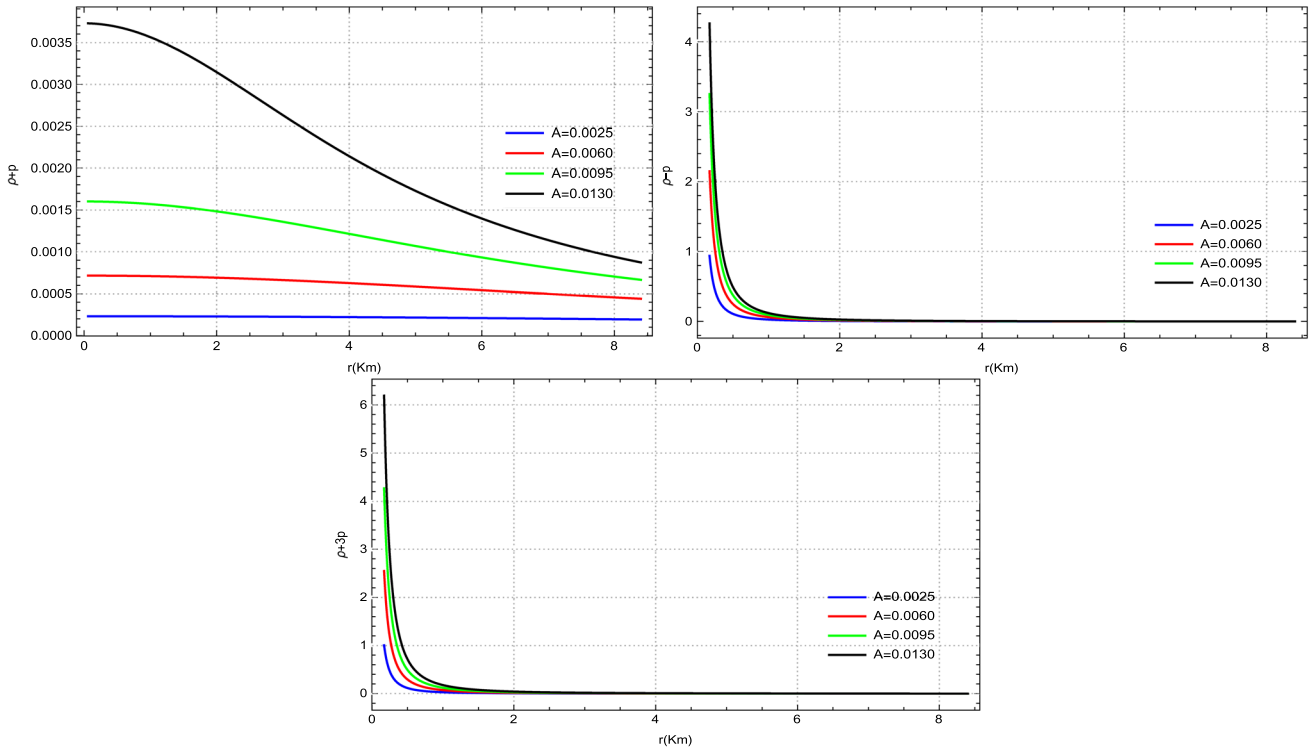

Fig. 7 Profile of Energy conditions corresponding to ordinary stellar matter against a radial function r

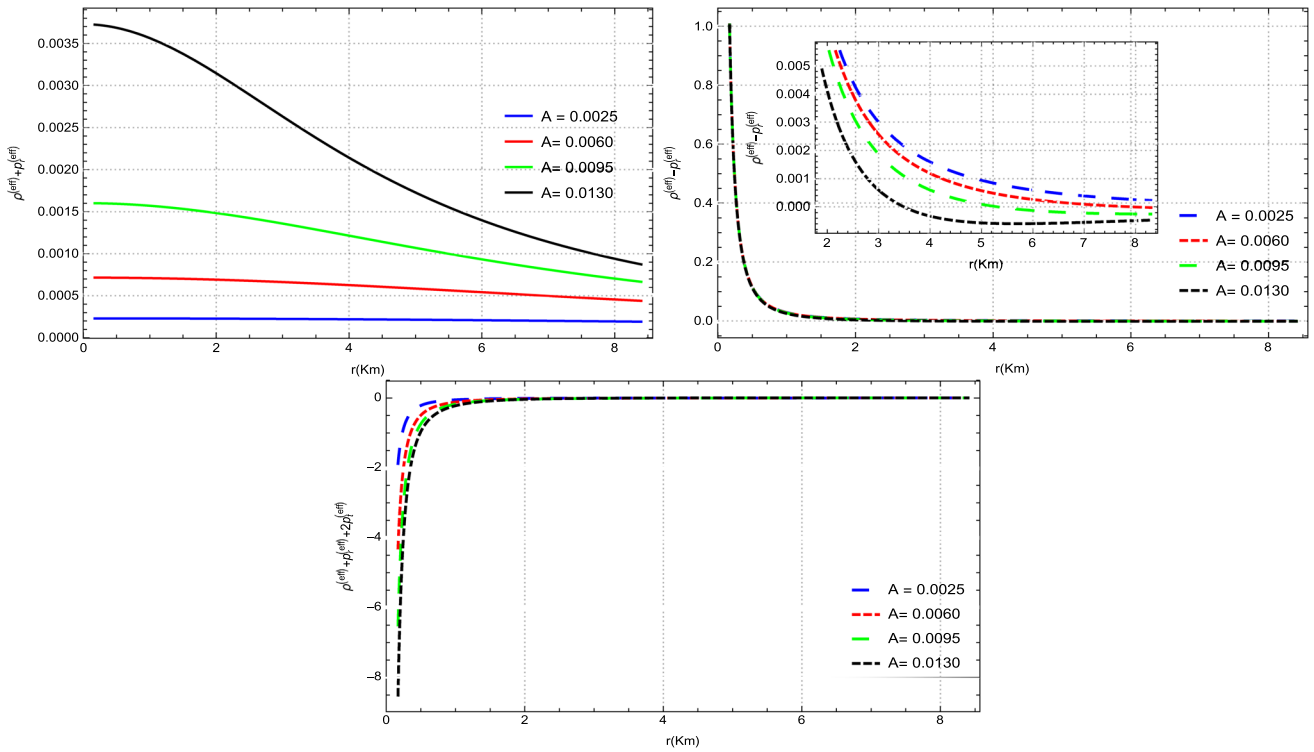

Fig. 8 Profile of Energy conditions corresponding to effective matter as a function of radial distance r

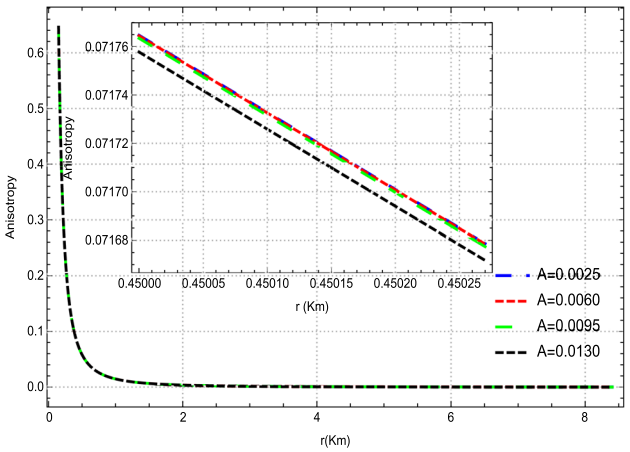

Fig. 9 Profile of pressure anisotropy vs r

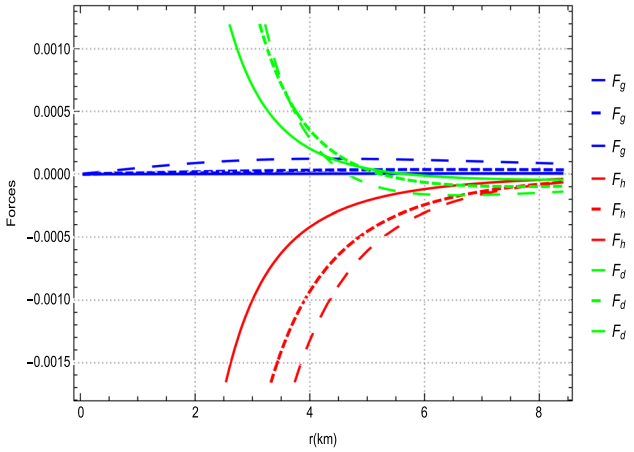

Fig. 10 Profile of equilibrium of forces vs radial distance r

- As shown in Fig. 9, the anisotropic stress remains positive and regular throughout the interior of the spherical dark energy star, corresponding to distinct intervals of A. The anisotropy of pressure decreases steeply from the center towards the stellar surface and reaches zero at approximately $r \sim R$. This behavior suggests the presence of a massive core surrounded by high-density regions, leading to significant anisotropic pressure variations driven by strong gravitational interactions, particularly in galactic halo regions. In such scenarios, the anisotropic pressure may transition to isotropic pressure at the surface, as traditionally observed in COs such as white dwarfs, neutron stars, and black holes.

5.2 Equilibrium of forces

Another feasible test for investigating the constancy and regularity of the presented spacetime geometry, based on the characteristics of a two-fluid distribution, is the equilibrium of forces. To confirm the potential stabilization of the equilibrium state of the model under the combined action of different forces acting on the system, we now define the Tolman–Oppenheimer–Volkoff (TOV) equation [123–125], which is expressed as follows:

$$\frac{a'}{2}\left(\rho^{(eff)}+p_r^{(eff)}\right)-\frac{2}{r}\left(p_t^{(eff)}-p_r^{(eff)}\right)+\frac{d}{dr}\left(p_r^{eff}\right)=0. \tag{42}$$

Here, the equation is decomposed into the following components

- The gravitational force (F_g), which deals for the inward pull due to gravity.
- The anisotropic force (F_a), arising from anisotropy of pressure in the stellar interior.
- The hydrostatic force (F_h), terming the gradient of pressure.

In its compact form, the TOV equation encapsulates the interplay between these forces, ensuring the equilibrium of dark energy COs. This framework provides a comprehensive understanding of the stability conditions and the physical dynamics governing compact stellar relativistic COs in these gravitational scenarios.

$$F_g+F_a+F_h=0. \tag{43}$$

More precisely,

$$F_g=\frac{a'}{2}\left(\rho^{(eff)}+p_r^{(eff)}\right), \tag{44}$$

$$F_a=-\frac{2}{r}\left(p_t^{(eff)}-p_r^{(eff)}\right)=-\frac{2\Pi}{r}, \tag{45}$$

$$F_h=\frac{d}{dr}\left(p_r^{eff}\right). \tag{46}$$

- Here, Π is the total measure of anisotropy of pressure. We examine the combined behavior of the prescribed forces acting on the proposed stellar system, as illustrated in Fig. 10. The interaction of these forces, analyzed for each value of the parameter A, reveals a realistic and stable configuration of the stellar geometry, ensuring hydrodynamic equilibrium at every interior point of the CO. This equilibrium arises from the effective counterbalancing of the gravitational and anisotropic dark forces against the hydrostatic force, which is negative throughout the system. Ultimately, this balance further supports the consistency and stability of our solutions in modeling dark energy COs.

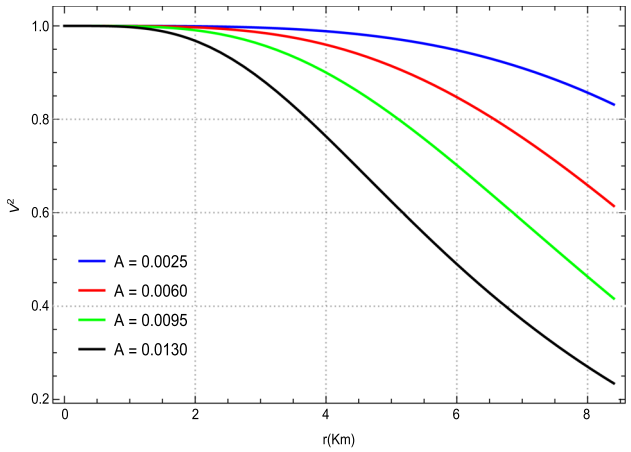

Fig. 11 Physical behavior of speed of sound (V^2) vs radial coordinate r

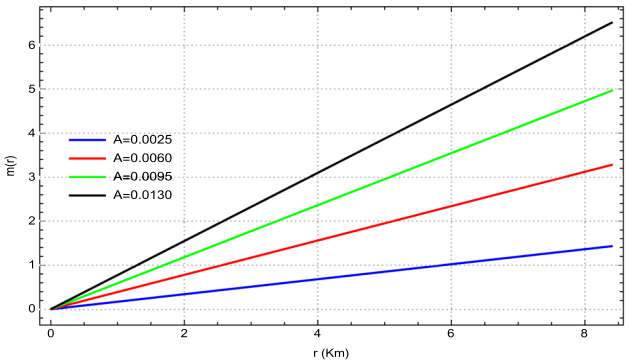

Fig. 12 Profile of mass function against a radial distance r

5.3 Causality condition

To ensure the stability of stellar astrophysical compact systems, another fundamental physical mechanism is evaluated using the causality condition, as established by Herrera's widely recognized cracking concept [126,127]. For a physically viable model, the speed of sound, $V^2 = \frac{dp}{d\rho}$, must satisfy the stability criterion: $V^2 = \frac{dp}{d\rho} \leq 1$. The speed of sound for our model solution is expressed as

$$V^2 = -\frac{-4B^2\left(-1+n^2\right)+4ABr^2\left(2-3n^2+n^4\right)+A^2r^4\left(-2+n^2\right)\left(-2+3n^2-n^4+4\sqrt{2-n^2}\left(1+\alpha\right)\right)}{\left(-1+n^2\right)\left(-2B+Ar^2\left(-2+n^2\right)\right)^2}. \quad (47)$$

- In Fig. 11, we analyze the physical behavior of the sound speed for our proposed dark star candidate. The sound speed exhibits a consistent and stable profile across the entire interior domain of the stellar body. Moreover, it remains within the required bounds, $0 \leq V^2 \leq 1$, adhering to the fundamental limits of stellar configurations. This confirms that our proposed model solution satisfies the causality condition, supporting the stabilized equilibrium formation of the dark energy CO.

5.4 Profile of mass function

We calculate the mass function by solving the differential equation (7), which is equivalent to the Misner-Sharp mass function [128] for a static and spherically symmetric dark stellar model. The profile of the effective mass function for our model sphere is expressed as

$$m(r) = 4\pi \int_0^r \rho^{(eff)} r^2 dr. \quad (48)$$

- The stellar mass is a realistic function of the radial coordinate r, exhibiting an increasing behavior from the core to the boundary, as shown in Fig. 12. The mass function demonstrates an evolutionary trend at every interior point of the compact stellar geometry, remaining bounded and attaining its maximum value as the radial coordinate r increases. These characteristics further affirm the reliability of the proposed model, which effectively describes an ultra-relativistic, dense dark energy CO, as discussed in [129].

6 Concluding remarks

In recent years, the diverse novel implications of stellar relativistic and astrophysical COs within the framework of the vanishing complexity factor formalism have garnered significant attention among various research groups. This interest stems from their stabilized and equilibrium configurations. In this context, we present exact analytical solutions for a static and spherically symmetric compact system by analyzing two-fluid distributions: ordinary stellar matter and dark energy, under the vanishing complexity factor formalism. To achieve this, we derived the Einstein field equations for these stellar relativistic fluid distributions by imposing the vanishing complexity factor condition. This condition effectively nullifies the complexity when the energy density inhomogeneity cancels out the pressure anisotropy or, equivalently, in isotropic systems. Using this approach, we generated spacetime solutions expressed through the relationships between the metric functions e^a and e^b. To close the system of equations, we adopted the Tolman-VI solution as the seed ansatz, alongside a linear dark energy EoS, which allowed

us to derive isotropic and anisotropic matter components for the gravitational field equations of stellar relativistic dark COs. Furthermore, we supported our proposed spacetime model both analytically and graphically by applying various physical constraints to the matter variables, such as the regularity of the metric variables, the physical plausibility of energy density and pressure terms (including their gradients), the viability of the state parameter, and the reliability of energy conditions. These analysis ensure the realistic configuration and potential adherence of the dark energy CO model. Additionally, we examined the stability and equilibrium state of the proposed model by analyzing pressure anisotropy, hydrostatic equilibrium of forces, speed of sound, and matter profiles. Moreover, we determined numerical values for the unknown constants and the dark energy coupling parameter (α) for various choices of the free parameter A, as given in Table 1. Notably, the estimated values of the dark energy coupling factor, corresponding to different values of A, reflect the exotic nature of the fluid distribution. This coupling effectively quantifies the amount of dark energy contributing to the structure and evolution of ultra-relativistic dark compact star candidates. The authenticity of the model is confirmed by the significant matter variables observed near the stellar core, which suggest that the spacetime geometry is composed of high-density regimes [116–118]. This validation demonstrates that our model solutions surpass previous results reported in [62]. Finally, several realistic features of our proposed results are elaborated as follows:

- **Acceptability of geometric components:** The analysis demonstrates that both geometric functions confirm the physical acceptability and realistic configuration necessary for the structure and evolution of dark energy CO. This conclusion is supported by their smooth matching with exterior geometries at the junction interface (see Fig. 1). Furthermore, the positive and non-singular behavior of the solutions suggests the stability of the model across the entire interior domain of the dark star candidate. Collectively, these attributes support the formulation of a stellar relativistic model for dark energy CO.
- **Potential viability of matter variables:** The physical adequacy of the proposed model has been evaluated by analyzing various matter profiles, including ordinary stellar fluid, dark energy, and their combined effective matter, as illustrated in **2**-**5**. These profiles exhibit well-consistent and feasible trends throughout the fluid sphere's composition. The trends reflect the behavior of energy densities, isotropic pressure, and the radial and transverse pressures of dark energy, along with their effective and first derivative functions. Notably, all profiles display maximum finite values near the stellar core, gradually decreasing with the radial coordinate r. In particular, the energy density associated with dark energy and the pressures of effective matter do not show any positive trends; rather, they remain decreasing functions of the radial coordinate r across the entire interior domain of the stellar body (see Fig. 3 (left panel) and Fig. 4 (right and lower panels)). These characteristics align with the expected behavior for a physically realistic and sustainable model of dark energy CO.
- **State parameter:** In addition, the physical plausibility of the state parameter has been examined to verify the realistic configuration of the dark spheroidal structure (see Fig. 6). This parameter exhibits a non-negative, bounded, and non-singular behavior at every interior point of the stellar spheroidal geometry. Furthermore, it is observed that the parameter remains within the required range, $0 \leq \omega \leq 1$, for $r < R$. Consequently, this condition ensures the stability and equilibrium configuration of the proposed dark star model.
- **Physical reliability of energy constraints:** In Figs. 7 and 8, we have analyzed the fundamental credibility of the fluid distribution in our proposed model by evaluating various energy conditions. These conditions establish the relationships between density and pressures, demonstrating the consistency and reliability of the stellar model. Specifically, the behavior of each plot in both profiles indicates that the energy conditions are well-satisfied and compatible with the stellar dark CO, thereby confirming its physical viability and dynamic equilibrium. However, the SEC associated with the effective components reveals an exotic influence characterized by the repulsive force of the dark energy fluid. This observation suggests that the effective SEC may be significantly influenced by strong gravitational interactions within such matter distributions.
- **Credibility via pressure anisotropy:** We have analyzed the impact of pressure anisotropy on the dark energy CO in Fig. 9. Each curve of pressure anisotropy, including the magnified view, exhibited a non-negative, regular trend. It demonstrated optimal behavior near the center and behaved as a moderately decreasing function of the radial distance r. This behavior reflects the evolution of a highly dense core region, leading to significant anisotropic pressure variations driven by strong gravitational interactions, particularly in stellar galactic halos. Under such conditions, the anisotropic pressure may transition to isotropic pressure at the surface, as commonly observed in COs such as white dwarfs, neutron stars, and black holes. This outcome further supports the stable and equilibrium configuration of the proposed dark star candidate.
- **Equilibrium of forces:** Despite the robust attributes of the model, we have also evaluated the feasibility of the stellar interior dark structure by examining the combined effects of three distinct forces, as illustrated in

Fig. 10. The physical significance of these forces was tested across the entire domain, revealing a strong agreement with the theoretical expectations and confirming the maintenance of a hydrodynamic equilibrium state at every interior point of the CO. This equilibrium arises from the effective counterbalancing of gravitational and anisotropic dark forces against the effective hydrostatic force, which remains negative throughout the system. Ultimately, this balance reaffirms the stability and physical acceptability of our model solutions in describing the configuration of the dark energy stellar structure.

- **Constancy via speed of sound:** From Fig. 11, we have analyzed the stability of our model by examining the sound speed as an essential characteristic. For a stable relativistic configuration, the speed of sound is expected to lie within the appropriate range $0 \leq V^2 \leq 1$. Our results confirm that this criterion is satisfied, clearly supporting the physical realism and viability of the proposed new dark energy CO.
- **Profile of mass function:** We have analyzed the evolutionary behavior of the mass function for our stellar model, as shown in Fig. 12. The mass profile is non-negative and exhibits a growing trend with the radial coordinate r. It remains bounded at every interior point and reaches its maximum value at the boundary surface. These trends validate the model's viability and effectively describe an ultra-compact dark energy star.

Funding Asifa Ashraf is very thankful to Prof. Wen Xiu Ma from the Department of mathematics, Zhejiang Normal University, for his kind support and help during this research. Further, Asifa Ashraf acknowledges grant No. YS304223918 to support his Postdoctoral Fellowship at Zhejiang Normal University.

Data Availability Statement This manuscript has no associated data. [Author's comment: This is a theoretical study and no experimental data is included.]

Code Availability Statement This manuscript has no associated code/software. [Author's comment: No numerical calculations are performed, hence no code/software is used.]

Funded by SCOAP[3].

References

1. A. Einstein, Sitzungsber. Preuss. Akad. Wiss. Berlin **25**, 844 (1915)
2. R. Sharma, S.D. Maharaj, Mon. Not. R. Astron. Soc. **375**, 1265 (2007)
3. M. Govender, S. Thirukkanesh, Astrophys. Space Sci. **358**, 39 (2015)
4. F. Tello-Ortiz, M. Malaver, Á. Rincón, Y. Gomez-Leyton, Eur. Phys. J. C **80**, 371 (2020)
5. S. Hansraj, L. Moodly, Eur. Phys. J. C **80**, 496 (2020)
6. E. Contreras, Z. Stuchlik, Eur. Phys. J. C **82**, 706 (2022)
7. J. Ospino, L.A. Núñez, Eur. Phys. J. C **80**, 166 (2020)
8. N.F. Naidu, M. Govender, S.D. Maharaj, Eur. Phys. J. C **78**, 48 (2018)
9. L. Herrera, Phys. Rev. D **97**, 044010 (2018)
10. L. Herrera, A. Di Prisco, J. Ospino, Phys. Rev. D **98**, 104059 (2018)
11. R. López-Ruiz, H.L. Mancini, X. Calbet, Phys. Lett. A **209**, 321 (1995)
12. R.G. Catalán, J. Garay, R. López-Ruiz, Phys. Rev. E **66**, 011102 (2002)
13. M.G.B. de Avellar, R.A. de Souza, J.E. Horvath, D.M. Paret, Phys. Lett. A **378**, 3481 (2014)
14. M.G.B. de Avellar, J.E. Horvath, Phys. Lett. A **376**, 1085 (2012)
15. J. Sañudo, A.F. Pacheco, Phys. Lett. A **373**, 807 (2009)
16. K.Ch. Chatzisavvas, V.P. Psonis, C.P. Panos, Ch.C. Moustakidis, Phys. Lett. A **373**, 3901 (2009)
17. L. Bel, Ann. Inst. Henri Poincaré **17**, 37 (1961)
18. A. García-Parrado, Gómez-Lobo, Class. Quantum Gravity **25**, 015006 (2008)
19. L. Herrera, J. Ospino, A. Di Prisco, E. Fuenmayor, O. Troconis, Phys. Rev. D **79**, 064025 (2009)
20. M. Sharif, I.I. Butt, Eur. Phys. J. C. **78**, 688 (2018)
21. M. Sharif, I.I. Butt, Eur. Phys. J. C **78**, 850 (2018)
22. R. Casadio, E. Contreras, J. Ovalle, A. Sotomayor, Z. Stuchlik, Eur. Phys. J. C **79**, 826 (2019)
23. S. Khan, S.A. Mardan, M.A. Rehman, Eur. Phys. J. C **79**, 1037 (2019)
24. S. Khan, S.A. Mardan, M.A. Rehman, Eur. Phys. J. C **82**, 620 (2022)
25. S. Khan, S.A. Mardan, M.A. Rehman, J. Cosmol. Astropart. Phys. **07**, 023 (2022)
26. P. León, C. Las Heras, Gen. Relativ. Gravit. **54**, 138 (2022)
27. G. Abbas, H. Nazar, Eur. Phys. J. C **78**, 510 (2018)
28. G. Abbas, H. Nazar, Eur. Phys. J. C **78**, 957 (2018)
29. H. Nazar, G. Abbas, Int. J. Geom. Methods Mod. Phys. **16**, 1950170 (2019)
30. G. Abbas, H. Nazar, Int. J. Geom. Methods Mod. Phys. **17**, 2050043 (2020)
31. G. Abbas, R. Ahmed, Astrophys. Space Sci. **364**, 194 (2019)
32. M. Zubair, H. Azmat, Phys. Dark Universe **28**, 100531 (2020)
33. H. Nazar, A.H. Alkhaldi, G. Abbas, M.R. Shahzad, Int. J. Mod. Phys. A **36**, 2150233 (2021)
34. M. Sharif, A. Majid, Eur. Phys. J. C **80**, 1185 (2020)
35. Z. Yousaf, M.Yu. Khlopov, M.Z. Bhatti, T. Naseer, Mon. Not. R. Astron. Soc. **495**, 4334 (2020)
36. Z. Yousaf, K. Bambab, M.Z. Bhatti, K. Hassan, New Astron. **84**, 101541 (2021)
37. S. Kiroriwa, J. Kumar, S.K. Maurya, S. Chaudhary, Chin. J. Phys. **89**, 1693 (2024)
38. R.S. Bogadi, M. Govender, S. Moyo, Eur. Phys. J. C **82**, 747 (2022)
39. S.K. Maurya, M. Govender, S. Kaur, R. Nag, Eur. Phys. J. C **82**, 100 (2022)

40. E. Contreras, E. Fuenmayor, G. Abellán, Eur. Phys. J. C **82**, 187 (2022)
41. S.K. Maurya, M. Govender, G. Mustafa, R. Nag, Eur. Phys. J. C **82**, 1006 (2022)
42. S.K. Maurya, G. Mustafa, S. Ray, B. Dayanandan, A. Aziz, A. Errehymy, Phys. Dark Universe **42**, 101284 (2023)
43. T.T. Smitha, S.K. Maurya, B. Dayanandan, G. Mustafa, Result Phys. **49**, 106502 (2023)
44. M. Al Shuali, S.K. Maurya, A. Al Abri, A. Al Ghufaili, B. Al Abri, B. Al Mayasi, A. Al Saadi, Int. J. Geom. Methods Mod. Phys. **20**, 2450015 (2023)
45. M. Al Habsi, S.K. Maurya, S. Al Badri, M. Al-Alawiya, T. Al Mukhaini, H. Al Malki, G. Mustafa, Eur. Phys. J. C **83**, 286 (2023)
46. S. Das, N. Sarkar, A. Das, S.K. Pal, Eur. Phys. J. C **84**, 817 (2024)
47. S. Das, M. Govender, R.S. Bogadi, Eur. Phys. J. C **84**, 13 (2024)
48. J. Andrade, D. Andrade, J. Phys.: Conf. Ser. **2796**, 012007 (2024)
49. Ksh.N. Singh, S.K. Maurya, S. Gedela, R.K. Bisht, J. High Energy Astrophys. **42**, 163 (2024)
50. Z. Yousaf, M.Z. Bhatti, T. Naseer, Phys. Dark Universe **28**, 100535 (2020)
51. S. Kaur, S.K. Maurya, S. Shukla, Phys. Scr. **8**, 105304 (2023)
52. S.K. Maurya, A. Errehymy, B. Dayanandan, S. Ray, N. Al-Harbi, A.H. Abdel-Aty, Eur. Phys. J. C **83**, 532 (2023)
53. M.K. Jasim, S.K. Maurya, A. Errehymy, A.K. Jassim, K.S. Nisar, A.H. Abdel-Aty, Chin. Phys. C **48**, 075108 (2024)
54. T. Naseer, M. Sharif, Prog. Phys. **72**, 2300254 (2024)
55. F.S.N. Lobo, Class. Quantum Gravity **23**, 1525 (2006)
56. M. Govender, S. Thirukkanesh, Astrophys. Space Sci. **358**, 39 (2015)
57. E.B. Gliner, Sov. J. Exp. Theor. Phys. **22**, 378 (1966)
58. J.M. Bardeen, in *Proceedings of the International Conference GR5, Tbilisi, USSR* (1968), p. 174
59. P. Bhar, F. Rahaman, Eur. Phys. J. C **75**, 41 (2015)
60. P. Bhar, Phys. Dark Universe **34**, 100879 (2021)
61. G. Abbas, S. Nazeer, M.A. Meraj, Astrophys. Space Sci. **354**, 449 (2014)
62. P. Rej, R.S. Bogadi, M. Govender, Chin. J. Phys. **87**, 608 (2024)
63. S.K. Maurya, Ksh.N. Singh, A. Aziz, S. Ray, G. Mustafa, Mont. Not. R. Astron. Soc. **527**, 5192 (2024)
64. G. Panotopoulos, Á. Rincón, I. Lopes, Phys. Lett. B **856**, 138901 (2024)
65. Á. Rincón, G. Panotopoulos, I. Lopes, Chin. J. Phys. **92**, 1373 (2024)
66. P. Beltracchi, P. Gondolo, Phys. Rev. D **99**, 044037 (2019)
67. S. Saklany, N. Pant, B. Pandey, Phys. Dark Universe **39**, 101166 (2023)
68. K.G. Sagar, N. Pant, B. Pandey, Phys. Dark Universe **38**, 101125 (2022)
69. S. Saklany, B. Pandey, N. Pant, Mod. Phys. Lett. A **37**, 2250182 (2022)
70. K.G. Sagar, B. Pandey, N. Pant, Astrophys. Space Sci. **367**, 72 (2022)
71. B. Dayanandan, T.T. Smitha, Chin. J. Phys. **71**, 683 (2021)
72. K.N. Singh, F. Rahaman, N. Pant, Ind. J. Phys. **96**, 209 (2022)
73. P. Rej, P. Bhar, Int. J. Geom. Methods Mod. Phys. **19**, 2250104 (2022)
74. M. Salti, O. Aydogdu, Ann. Phys. **455**, 169359 (2023)
75. A. Majeed, H. Nazar, G. Abbas, Chin. J. Phys. **86**, 530 (2023)
76. A. Majeed, G. Abbas, A. Siddiqa, A. Ashraf, H. Nazar, A. Abd-Elmonem, Phys. Dark Universe **46**, 101705 (2024)
77. P. Bhar, Astrophys. Space Sci. **357**, 46 (2015)
78. M.R. Shahzad, G. Abbas, Astrophys. Space Sci. **365**, 147 (2020)
79. G. Abbas, H. Nazar, Ann. Phys. **424**, 168336 (2021)
80. H. Nazar, G. Abbas, Adv. Astron. **2021**, 6698208 (2021)
81. R.C. Tolman, Phys. Rev. **55**, 364 (1939)
82. S. Biswas, D. Shee, S. Ray, F. Rahaman, B.K. Guha, Ann. Phys. **409**, 167905 (2019)
83. M. Jasim, D. Deb, S. Ray, Y. Gupta, S.R. Chowdhury, Eur. Phys. J. C **78**, 603 (2018)
84. S. Biswas, D. Shee, B.K. Guha, S. Ray, Eur. Phys. J. C **80**, 175 (2020)
85. A. Majeed, G. Abbas, M.R. Shahzad, New Astron. **102**, 102039 (2023)
86. S. Hansraj, A. Banerjee, Phys. Rev. D **97**, 104020 (2018)
87. P. Bhar, K.N. Singh, F. Tello-Ortiz, Eur. Phys. J. C **79**, 922 (2019)
88. A. Majid, M. Sharif, Universe **6**, 124 (2020)
89. M.F. Shamir, I. Fayyaz, Int. J. Geom. Methods Mod. Phys. **17**, 2050140 (2020)
90. T. Naz, M.F. Shamir, Int. J. Mod. Phys. A **35**, 2050040 (2020)
91. P. Rej, P. Bhar, M. Govender, Eur. Phys. J. C **81**, 316 (2021)
92. M. Javed, G. Mustafa, M.F. Shamir, New Astron. **84**, 101518 (2021)
93. J. Andrade, E. Contreras, Eur. Phys. J. C **81**, 889 (2021)
94. P. Bhar, S. Das, B.K. Parida, Int. J. Geom. Methods Mod. Phys. **19**, 2250095 (2022)
95. P. Bhar, Chin. J. Phys. **83**, 61 (2023)
96. M. Aslam, A. Malik, Ann. Phys. **472**, 169854 (2025)
97. C. Arias, E. Contreras, E. Fuenmayor, A. Ramos, Ann. Phys. **436**, 168671 (2022)
98. A. Rincon, G. Panotopoulos, I. Lopes, Universe **9**, 72 (2023)
99. A. Rincon, G. Panotopoulos, I. Lopes, Eur. Phys. J. C **83**, 116 (2023)
100. J. Ospino, L.A. Nunez, Eur. Phys. J. C **80**, 166 (2020)
101. C.R. Ghezzi, Astrophys. Space Sci. **333**, 437 (2011)
102. F. Rahaman, R. Maulick, A.K. Yadav, S. Ray, R. Sharma, Gen. Relativ. Gravit. **44**, 107 (2012)
103. C.R. Ghezzi, Phys. Rev. D **72**, 104017 (2005)
104. B. Wang, E. Abdalla, F. Atrio-Barandela, D. Paṽon, Rep. Prog. Phys. **79**, 096901 (2016)
105. B. Dayanandan, T.T. Smitha, Chin. J. Phys. **71**, 683 (2021)
106. J. Yoo, Y. Watanabe, Int. J. Mod. Phys. D **21**, 1230002 (2012)
107. M. Li, S.X.-D. Wang, Y. Wang, Front. Phys. **8**, 828 (2013)
108. S. Wang, Y. Wang, M. Li, Phys. Rep. **696**, 1 (2017)
109. P. Beltracchi, P. Gondolo, Phys. Rev. D **99**, 044037 (2019)
110. M. Demianski, E. Lusso, M. Paolillo, E. Piedipalumbo, G. Risaliti, Front. Astron. Space Sci. **7**, 521056 (2020)
111. M.F.A.R. Sakti, A. Sulaksono, Phys. Rev. D **103**, 084042 (2021)
112. K. Schwarzschild, Sitzbcr. Press. Akad. Wiss. Berlin, 189 (1916)
113. G. Darmois, Ḿemorial des sciences mathématiques XXV (Gauthier-Villars, 1927)
114. W. Israel, Nuovo Cim. B **44**, S10 (1966). [Erratum: Nuovo Cim. B **48**, 463 (1967)]
115. P. Bhar, P. Rej, New Astron. **100**, 101990 (2023)
116. R. Ruderman, Annu. Rev. Astron. Astrophys. **10**, 427 (1972)
117. N.K. Glendenning, *Compact Stars: Nuc. Phys. Particle Physics and General Relativity* (Springer, New York, 1997), p. 468
118. M. Herzog, F.K. Röpke, Phys. Rev. D **84**, 083002 (2011)
119. P. Bhar, Prog. Phys. **71**, 2300074 (2023)
120. C.W. Misner, D.H. Sharp, Phys. Rev. **136**, B571 (1964)
121. D. Shee, S. Ghosh, F. Rahaman, B.K. Gupta, S. Ray, Astrophys. Space Sci. **362**, 114 (2017)
122. H. Quevedo, Phys. Rev. D **39**, 2904 (1989)
123. J.R. Oppenheimer, G.M. Volkoff, Phys. Rev. **55**, 374 (1939)
124. J. Ponce de León, Gen. Relativ. Gravit. **19**, 797 (1987)
125. J. Ponce de León, Gen. Relativ. Gravit. **25**, 1123 (1993)
126. L. Herrera, Phys. Lett. A **165**, 206 (1992)
127. H. Abreu, H. Hernandez, L.A. Nunez, Class. Quantum Gravity **24**, 4631 (2007)
128. C. Misner, D. Sharp, Phys. Rev. **136**, B571 (1964)
129. P. Bhar, Astrophys. Space Sci. **359**, 41 (2015)